# First-principles study of adhesion at Cu/$SiO_2$ interfaces

Kazutaka Nagao,[1,*] J. B. Neaton,[2] and N. W. Ashcroft[1]
[1]*Cornell Center for Materials Research, and Laboratory of Atomic and Solid State Physics, Cornell University, Clark Hall, Ithaca, New York 14853-2501, USA*
[2]*Department of Physics and Astronomy, Rutgers University, Piscataway, New Jersey 08854-8019, USA*
(Received 21 April 2003; revised manuscript received 2 July 2003; published 8 September 2003)

The structural, electronic, and adhesive properties of Cu/$SiO_2$ interfaces are investigated using first-principles density-functional theory within the local density approximation. Interfaces between fcc Cu (001) and $\alpha$-cristobalite (001) slabs with different surface stoichiometries are considered. Interfacial properties are found to be sensitive to the choice of the termination and the interfacial oxygen density is the most important factor influencing the strength of adhesion. For oxygen-rich interfaces, the O atoms at the interface substantially rearrange after the deposition of Cu layers, suggesting the formation of Cu-O bonds. The large structural rearrangement, site-projected local densities of states, and changes in electron density indicate hybridization between Cu-*d* and O-*p* states at the interface. As oxygen is systematically removed from the interface, less rearrangement is observed, reflecting less hybridization and weaker adhesion. Computed adhesion energies for each of the interfaces are consistent with the observed structural and bonding trends, leading to the largest adhesion energy in the oxygen rich cases. The adhesion energy is also calculated between Cu and $SiO_2$ substrates terminated with hydroxyl groups, and adhesion of Cu to these substrates is found to be considerably reduced. This work supports the notion that Cu films can adhere well to hydroxyl-free $SiO_2$ substrates should oxygen be present in sufficient amounts at the interface.

DOI: 10.1103/PhysRevB.68.125403 PACS number(s): 68.35.−p, 73.20.−r, 68.47.Gh

## I. INTRODUCTION

Adhesion of thin metal films to glass substrates has continued to be the subject of intense study for many years because of its importance to the large-area electronics industry. Copper in particular, a noble metal with high bulk thermal and electrical conductivities, and an apparently low electromigration rate,[1] is an excellent candidate for interconnects in integrated circuitry on dielectric substrates, and thus the formation of a strong and highly reliable interface between copper and glass has been an issue of primary importance. Unfortunately, Cu films are often reported to bind rather poorly to oxide-based glass substrates,[2–15] and films that do adhere at room temperature can show diminished adhesivity after thermal cycling,[8,12] an effect often attributed to differences of thermal expansion between Cu and the oxide substrate.[8] In many studies, poor bonding is frequently explained by noting that since Cu does not reduce $SiO_2$, a graded oxide layer facilitating the adhesion is unable to form. Chemically, copper possesses a half-empty *s* shell and a reasonably tightly bound and filled *d* shell, and thus is less reactive than aluminum and many transition metal films,[2] which oxidize well and are observed to adhere more reliably. Thus it is not surprising that adhesion is often improved experimentally by applying transition metal intermediary layers[6,8] prior to Cu film deposition, or alloying the Cu films with small amounts of Mg or Al.[4,5,9–12]

Adhesion of copper films to oxide glasses is, of course, expected to be highly sensitive to the temperature, oxygen partial pressure, and the condition of the glass surface prior to deposition. A common feature of many studies of Cu films on glass is that they were performed under conditions amenable to surface passivation either before or during deposition of the copper film. However, Cu films sputtered under high purity conditions in a vacuum *do* adhere to glass substrates.[5,7,8] In particular, Ohmi *et al.*[7] demonstrated robust adhesion of copper to glass after removing hydroxyl (OH) groups from the interface *in situ* just prior to deposition. This suggests that dangling bonds at moisture-free glass surfaces would be readily saturated by Cu-O bonds.

Glasses important to industry can be chemically complex, often containing a substantial amount (perhaps ~30%) of aluminum, boron, and other alkaline earth elements. Their primary component, however, is almost always $SiO_2$, which by itself forms one of the simplest glasses, amorphous silica ($a$-$SiO_2$). In the interest of simplifying the chemistry, we shall restrict our focus to chemically pure $SiO_2$ glasses for the duration of this study. Amorphous silica has no long range order yet remarkably, on length scales comparable to a Si-O bond, it is nearly perfectly ordered: the bond length does not vary appreciably from 1.61 Å; each Si atom is tetrahedrally coordinated with O atoms, and the bonds are primarily of a covalent nature.[16,17] At length scales between 5 and 8 Å, minimal variations in O-Si-O and Si-O-Si bond angles result in an appreciable degree of intermediate range orientational order.[16,17] Previous work using molecular dynamics considered both bulk vitreous silica and silica surfaces.[18–22] Much of it was based on semiempirical potentials,[18–21] which though able to simulate systems large enough to correctly capture the effects of the intermediate range orientational order, are expected to be far less accurate when local conditions deviate from those in the bulk, such as they do at surfaces or interfaces.

Since microscopically adhesion is related to the strength of the electronic bond between atoms at the interface, the *local* electronic structure at the interface will play an important role in understanding the reactivity of the metal with the oxide substrate. A first-principles treatment would therefore

 ©2003 The American Physical Society

be most appropriate for examining the nature of local bonding at an ideal interface between the two systems, and indeed this approach has proved insightful in the past for studying adhesion between metal films and insulating substrates.[23–26] Previous first-principles work on the $\alpha$-quartz surface[22] observed significant changes in bonding near the surface; to our knowledge, however, the effects of metallic overlayers on $SiO_2$ surface geometries and electronic properties have yet to be examined from first principles.

In this article, we assess the degree to which the chemical bonding at atomically sharp interfaces reflects the empirical trends in the adhesion of metallic contacts to glass substrates through study of a simplified system, Cu monolayers on $\alpha$-cristobalite. $\alpha$-cristobalite is a crystalline $SiO_2$ polymorph which although ordered does possess a density quite close to that of $a$-$SiO_2$.[27] Adhesion is studied as a function of oxygen surface coverage from first principles, using density functional theory within the local density approximation (LDA).[28] Our methods allow us to elucidate the role of local chemistry in binding the film to glass, but require us to neglect its inherent long-range disorder and also, to a limited extent, its intermediate-range orientational disorder. Since we are chiefly interested in the local bonding properties, which are expected to be the same for both amorphous and crystalline silica, the loss of disorder is acceptable. We summarize the method and approximations used here in Sec. II; in Sec. III we describe the relaxed $1\times1$ $\alpha$-cristobalite (001) surfaces considered here, which include both stoichiometric and non-stoichiometric surface terminations, and which were chosen so as to reflect different possible oxygen coverages that may result from different deposition conditions. In Sec. IV, we detail results of atomic relaxation of Cu (001)/$SiO_2$ interfaces, where the adhesion is found to be critically sensitive to oxygen density at the substrate surface, and where relatively strong bonding is reported for oxygen-rich surfaces. The effect of hydroxyl groups as a surface passivator is also briefly considered by calculating adhesion energies between copper monolayers and a hydroxyl-terminated $SiO_2$ surface. After discussing our results and their implications, we provide concluding remarks in Sec. V.

## II. METHODOLOGY

### A. Computational details

Our first-principles density-functional calculations are carried out within the LDA, using the correlation energy of Ceperley and Alder,[29] as implemented within the Vienna *ab initio* Simulation Program[30–32] (VASP). We use a plane-wave basis set with a 29 Ry cutoff, and ultrasoft pseudopotentials[33,34] for Cu and H, projector augmented-wave potentials[35,36] for O, and a norm-conserving pseudopotential[37] for Si. The Monkhorst-Pack $\boldsymbol{k}$-point mesh is chosen so that $n_k = 3\times3\times1$ for the 5 Å$\times$5 Å$\times$30 Å supercell which is used in this work. Also, we make use of a Fermi-distribution smearing with the temperature of $k_BT \sim 0.2$ eV to facilitate rapid convergence. These computational conditions provide good convergence of the structure, density of states, and energy differences given here, and are used throughout this work unless otherwise stated.

TABLE I. Lattice constants of Cu and $\alpha$-cristobalite observed in experiment and LDA calculation (Ref. 39). Wyckoff positions, two Si-O bond lengths, and four O-Si-O bond angles are also shown for $\alpha$-cristobalite; the Si Wyckoff position $(4a)$ is shown as $(u,u,0)$ and the O Wyckoff position $(8b)$ as $(x,y,z)$. The experimental data are taken from Refs. 38 and 40 for copper and $\alpha$-cristobalite, respectively.

| | | Experiment | This work (LDA) |
|---|---|---|---|
| Cu | $a$ (Å) | 3.615 | 3.532 |
| | $\sqrt{2}a$ (Å) | 5.112 | 4.995 |
| $\alpha$-cristobalite | $a$ (Å) | 4.972 | 4.975 |
| | $c$ (Å) | 6.922 | 6.907 |
| | $u$ (Si) | 0.3003 | 0.3005 |
| | $x$ (O) | 0.2392 | 0.2389 |
| | $y$ (O) | 0.1044 | 0.1058 |
| | $z$ (O) | 0.1787 | 0.1801 |
| | Si-O (Å) | 1.6026 | 1.6056 |
| | Si-O (Å) | 1.6034 | 1.6062 |
| | O-Si-O (°) | 109.0 | 108.3 |
| | O-Si-O (°) | 110.0 | 109.9 |
| | O-Si-O (°) | 108.2 | 108.8 |
| | O-Si-O (°) | 111.4 | 111.7 |

It should be mentioned that the $\boldsymbol{k}$-point sampling discussed above is not entirely sufficient for study of the bulk properties of copper. In fact, the total energy of bulk copper obtained with this sampling is converged to only about 0.02 eV per Cu atom. However, a sparser mesh turns out to be adequate for this study since energy differences are converged. To demonstrate, we increased our sampling to $n_k = 4\times4\times1$ for the supercell mentioned above, recalculated total energies and forces, and found that the resulting difference in adhesion energy is less than 4% even in the largest case.

### B. Bulk properties of constituent systems

Copper crystallizes in the fcc structure under normal conditions and its lattice constant is 3.615 Å at 291 K.[38] The LDA underestimates this lattice constant as is well known, and we obtain 3.532 Å for the equilibrium value as shown in Table I, in agreement with a previous LDA study.[41] At equilibrium we find $a = 4.975$ Å and $c = 6.907$ Å for the tetragonal cell of bulk $\alpha$-cristobalite (the $P4_12_12$ structure), in excellent agreement with experiment[40] and previous LDA calculations.[42,43] Further, the computed Si-O bond length ($\sim 1.606$ Å) is remarkably close to experiment ($\sim 1.603$ Å), and the calculated O-Si-O bond angle is near the tetrahedral ideal value, also in-line with measurement.[40] Conveniently, the choice of $\alpha$-cristobalite circumvents spurious lattice mismatch when considering the interfaces with Cu overlayers: Compare the lattice constant $a$ of $\alpha$-cristobalite with $\sqrt{2}a$ of Cu in Table I. Since the generalized gradient approximation (GGA) (Ref. 44) has been largely unsuccessful in predicting structural parameters in agreement with experiment for $SiO_2$ polymorphs,[43] we use the LDA throughout this work and reserve a complete

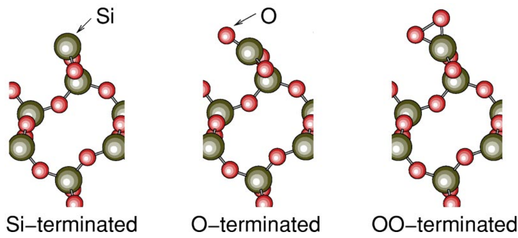


FIG. 1. (Color online) Relaxed structures of the $\alpha$-cristobalite (001) surfaces.

numerical comparison between the LDA and GGA for a future study.

### III. (001) SURFACES OF $\alpha$-CRISTOBALITE $SiO_2$

As a starting point, we consider an $\alpha$-cristobalite slab consisting of five $SiO_2$ layers, the thickness of which is $\sim$8.3 Å. Translational symmetry is removed along the $c$ axis, defining two different (001) surfaces perpendicular to this axis. We embed this $\alpha$-cristobalite slab, along with about 20 Å of vacuum, within a supercell having dimensions of 5 Å$\times$5 Å$\times$30 Å. The oxygen density at the top of our $SiO_2$ slab is then changed to mimic different substrate terminations. Two nonbridging oxygen atoms terminate the bottom of the slab, and two additional H atoms are attached to the oxygens to remove dangling bonds. Forces on the atoms are computed using the Hellmann-Feynman theorem, and the positions of atoms are then updated until the total energy reaches a minimum. The oxygen atoms at the bottom surface, terminated by hydrogens, are fixed at their bulk positions in order to reduce size effects owing to the finite thickness of the $SiO_2$ slab, though the positions of each of the hydrogen atoms are permitted to relax. Previous first-principles calculations of $\alpha$-quartz surfaces[22] and model $Si/SiO_2$ interfaces[45] have indicated that about 5 Å away from the interface, the local structural and electronic properties of the slab are bulklike, and thus the size of our slab is sufficient to approximate both surface and bulk features.

Figure 1 presents views of the relaxed $\alpha$-cristobalite (001) surfaces. Supercells with slabs having three different surface terminations are considered in this work, which we label as Si, O, and OO terminated. The Si-terminated slab contains five $SiO_2$ units together with two bottom hydrogens; the O-terminated slab is identical to the Si-terminated one except that the dangling surface oxygen atom is added; the OO-terminated slab is again a modification of the Si-terminated slab in which two oxygens are added to the surface. Bond lengths and angles are not expected to remain bulklike at the surface, where the choice of termination can leave nonbridging oxygens with dangling bonds (e.g., in the OO-terminated cases). Indeed, we find that relaxation significantly changes the Si-O bond lengths within two atomic layers from the surface for all terminations considered, and the nature of these changes is strongly dependent on the termination. In the Si-terminated case, the additional charge carried by the dangling Si bonds forces the Si surface atom above the plane of the surface; as a result the Si-O bonds supporting it from below elongate slightly to 1.64 Å. In the O-terminated case, the surface O atom, bonded to only one other Si, relaxes downward *into* the surface, and its bond length decreases by more than 5% from 1.6 to 1.5 Å. In the OO-terminated case, in some contrast to the Si- and O-terminated slabs, the Si-O bond lengths remain essentially the same as bulk. But the distance between O neighbors on the surface is also 1.6 Å, which is very small compared with typical bulk O second neighbor distances of 2.7 Å. Thus O atoms may evidently saturate dangling bonds through bonding with neighboring O atoms at this surface.

As expected, the total cohesive energies of the supercells decrease substantially with each additional O atom: adding one oxygen atom or two oxygen atoms lowers the cohesive energy by $\sim$7.1 or $\sim$11.3 eV per surface Si, respectively. Since the energy required to break the $O_2$ bond is nearly 5 eV per molecule, this energy comparison suggests that the OO-terminated surface may be the most stable of the three terminations, and the O-terminated surface the second. Evidently our first-principles calculations are consistent with the intuition that glass surfaces should be oxygen rich.

### IV. $SiO_2$ INTERFACES: RESULTS AND DISCUSSION

#### A. Interfacial structure

We now add five (001) Cu layers to each of the fully relaxed (001) $\alpha$-cristobalite surfaces, obtained as discussed above in Sec. III. We note that Ohmi *et al.*[7] has observed that Cu films, when grown initially in a (111) orientation, transform to (001) through thermal annealing. This indicates that (001)-oriented Cu films are stable on silica, and thus our supercell choice is expected to be relevant to actual $Cu/a$-$SiO_2$ interfaces.

The (001) Cu layers are initially positioned on the surface so that a Cu atom in the lowest monolayer lies on the former symmetry axis of the $\alpha$-cristobalite slab. The length of the supercell lattice vector normal to the surface (the $c$ axis) is fixed to 30 Å as in Sec. III, a value we find to be large enough to accommodate up to five additional Cu layers while keeping the interactions between the surfaces in neighboring supercells minimal. Each monolayer in our supercell contains four Cu atoms, and before relaxation each Cu atom has four intralayer neighbors at a distance of 2.5 Å. The lattice parameter of the $1\times1$ surface of $\alpha$-cristobalite is well matched to that of the $\sqrt{2}\times\sqrt{2}$ surface of copper as shown in Table I (the mismatch is less than 1%). The small lattice mismatch is artifact of our approximate treatment of amorphous silica as crystalline. In reality, stress induced by lattice matching is relieved through formation of defects and/or dislocations. (In the case of a truly amorphous substrate, stress may also be overcome through surface reconstruction, a complexity we neglect in the present work.)

All atomic positions in the supercell are again relaxed except for the bottom O atoms, and Fig. 2 shows the optimized structures of the interfaces for each termination. The most significant reconstruction at the interface is observed in the OO-terminated case. The O-O bond observed at the free $\alpha$-cristobalite surface in Fig. 1 is broken by the deposition of copper, and the O-Si-O angle is changed from 59° to 104° with the Si-O bond lengths kept almost constant. This large

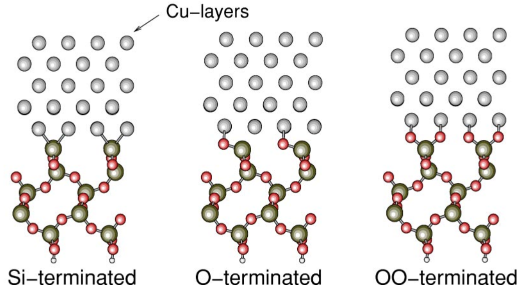


FIG. 2. (Color online) Relaxed structures of the Cu/$\alpha$-cristobalite (001) interfaces.

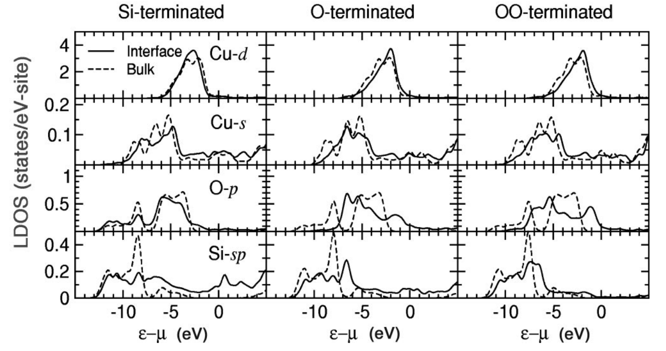


FIG. 3. Local density of states (LDOS) projected by site and angular momentum. The solid lines show the LDOS of atoms at (or near) the interfaces, and the dashed lines show those of atoms in the middle of the slabs (the LDOS of an approximate bulk material). When computing the LDOS, a Gaussian smearing method is used with $\sigma=0.2$ eV. The sphere sizes of each atom are taken as 1.11 Å for Si, 0.73 Å for O, and 1.38 Å for Cu.

rearrangement would indicate bond formation between interfacial O and Cu atoms, suggesting good chemical adhesion between the oxide substrate and the Cu film. Each interfacial O atom has two Cu neighbors, and the Cu-O bond lengths are computed to be $\sim 1.9$ Å, strikingly similar to Cu-O distances found in cuprates,[46] where each copper atom is coordinated by four oxygens and considered to be in a $Cu^{2+}$ state. Similar Si-O and Cu-O bond lengths are observed at the interface between O-terminated surfaces and Cu monolayers, although the Si-O-Cu angles are smaller than in the OO-terminated case by $\sim 15°$, as can be seen in Fig. 2. The magnitude of the reconstruction at the O-terminated/Cu interface is less than that at the OO-terminated/Cu interface.

The interface between the Si-terminated substrate and Cu is completely different from either of the oxygen terminated interfaces. In this case, the interfacial Si atom possesses four Cu neighbors, each with bond length $\sim 2.4$ Å, and there is negligible atomic rearrangement, implying more metalliclike bonding.

### B. Electronic properties

To investigate further the bonding properties of each interface discussed above, we compute the site-projected local density of states (LDOS) for atoms near the interfaces, and compare them with those obtained for bulklike atoms deeper inside the slabs; the LDOS are shown together for each interface in Fig. 3. In the OO-terminated case, significant hybridization is observed between Cu-*d* and O-*p* states just below the Fermi level. A key feature is the slight bump in the O-*p* LDOS, lying about 1 eV below the Fermi energy, which becomes progressively smaller with decreasing O content at the interface, and nearly vanishes in the Si-terminated case. [Partial wave decomposition of wave functions near the Fermi level confirms the existence of $p(\mathrm{O})$-$d(\mathrm{Cu})$ hybridization at the interface.] Evidently, this hybridization is responsible for the significant reconstruction at the OO interface. It is worth pointing out that as the number of O atoms at the interface is decreased, the Si-*sp* LDOS around the Fermi energy increases, and the interfacial bonding takes on a more metallic character. This behavior results from the hybridization of Si-*sp* states with the itinerant Cu-*s* states around the Fermi energy. In addition, we observe the bandgap computed within the LDA (an underestimate of the true bandgap) opens and gradually approaches its bulk LDA value for LDOS in the middle of the $SiO_2$ slab, confirmation that our slab exhibits approximate bulk behavior away from the interface.

To examine the degree to which changes in structural and bonding properties are confined to the interface, and to observe the mixing between the electronic states of the $SiO_2$ substrate and the Cu layers in more detail, we calculate the density difference,

$$\langle \delta n(z)\rangle=\langle n_{\mathrm{IF}}(z)\rangle-[\langle n_{\mathrm{SiO_2}}(z)\rangle+\langle n_{\mathrm{Cu}}(z)\rangle],$$

where $\langle n_{\mathrm{IF}}(z)\rangle$, $\langle n_{\mathrm{SiO_2}}(z)\rangle$, and $\langle n_{\mathrm{Cu}}(z)\rangle$ are the densities of the Cu/$SiO_2$ interface, the $SiO_2$ substrate, and the Cu layers, respectively, averaged over the *xy* plane (parallel to the interface). To obtain $\langle n_{\mathrm{SiO_2}}(z)\rangle$ ($\langle n_{\mathrm{Cu}}(z)\rangle$), we simply remove the Cu layers ($SiO_2$ substrate) from the fully relaxed interface in the supercell, and then recalculate the electronic structure self-consistently keeping the atoms fixed. The quantity $\langle \delta n(z)\rangle$ thus indicates the change in electron density resulting from chemical bonding between the Cu layers and the $SiO_2$ substrate. (To simplify the analysis, we are neglecting additional changes stemming from the atomic rearrangements at the free surfaces of $SiO_2$ and Cu.) The results of calculations of the $\langle \delta n(z)\rangle$ appear in Fig. 4. The $\langle \delta n(z)\rangle$ in the OO-terminated case most prominently deviates from zero around the interface, reflecting significant charge transfer between the two slabs. The charge transfer in the O- and Si-terminated cases is comparatively much smaller. In particular, in the Si-terminated case, the depletion of the density in the vicinity of the lowest Cu layer is not so drastic, suggesting that the localized Cu-*d* states have less influence on the bonding around the interface.

In summary, through the dependence of the partial DOS on the O density and interface structure, and through the changes in the atomic structure and charge density at the interface, we observe $p(\mathrm{O})$-$d(\mathrm{Cu})$ hybridization and the development of Cu-O bonds at the Cu/$SiO_2$ interface.

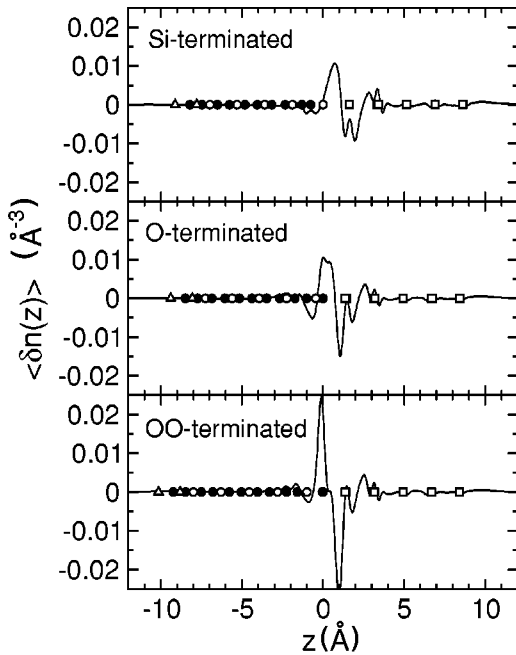


FIG. 4. Change in electron density $\langle \delta n(z) \rangle$ (see text) as a function of the depth $z$ from the substrate surface. The positions of each atom are designated by open circles for Si, solid circles for O, open squares for Cu, and open triangles for H.

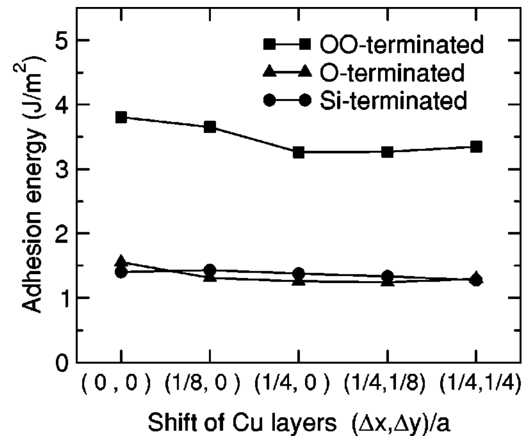


FIG. 5. Adhesion energy as a function of the position of Cu layers in the $xy$ plane calculated for five different initial positions and for each of the three terminations. Each point is obtained by translating Cu layers [initially positioned on the substrate as described in Sec. IV A $(\Delta x=0,\Delta y=0)$] in the $xy$ plane by $(\Delta x,\Delta y)$ and then fully relaxed. The abscissa (which quantifies the magnitude of the shift of Cu layers) is scaled by the supercell lattice parameter $a=5$ Å.

### C. Quantitative analysis of adhesion

To assess the adhesive strength of the interfaces quantitatively, we have calculated the ideal work of separation, or *adhesion energy*, per unit area $W$ from

$$W \equiv (E_{SiO_2}+E_{Cu}-E_{IF})/A,$$

where $E_{SiO_2}$, $E_{Cu}$, and $E_{IF}$ are the energies of the isolated $SiO_2$ substrate, Cu layers, and Cu/$SiO_2$ interface in the supercell, respectively, and $A$ is the area. Physically, the adhesion energy $W$ is the work per unit area required to separate the interface into the Cu layers and the $SiO_2$ substrate within a microcanonical process, and it can be considered a measure of the strength of the adhesion. For the purposes of comparison, all energies are calculated using supercells of the same size (5 Å×5 Å×30 Å) independent of whether it contains Cu layers, any of the $SiO_2$ substrates, or Cu/$SiO_2$ interfaces. Table II lists the adhesion energy for each case. The adhesion energy in the OO-terminated case turns out to be much larger than those in the O- and Si-terminated cases, and comparable to values previously computed for other metal-dielectric interfaces, such as Co/TiC (Ref. 23) and Nb/$Al_2O_3$ (Ref. 24). We note that the computed adhesion energy for the OO-terminated case, $\sim$4 J/m$^2$, are consistent with values obtained experimentally by Kriese *et al.*[6] for 100 nm thick films of Cu on $SiO_2$ using an indentation technique. In summary, the magnitudes of adhesion energies computed here for each of the three different interfaces reflect the trends witnessed above in their structural and bonding properties.

TABLE II. Adhesion energies (ideal work of separation) $W$ of Cu/$\alpha$-cristobalite (001) interfaces computed within the LDA.

| | $W$ (J/m$^2$) |
|---|---|
| Si terminated | 1.406 |
| O terminated | 1.555 |
| OO terminated | 3.805 |

#### *1. Local atomic structure*

At this point, it is meaningful to investigate further a drawback of using crystalline $\alpha$-cristobalite to model the amorphous substrate. When Cu layers are placed on an amorphous $SiO_2$ substrate, different local atomic configurations are possible at the interfaces because of the nonperiodicity of glass. A principal simplification of our model is the imposition of translational symmetry: we are unable to directly assess the difference between the adhesive properties of crystalline substrates and those of amorphous substrates. We are, however, able to investigate the sensitivity of our calculated adhesion energies to changes in local atomic structure. As a first step, we compute the influence of the position of Cu layers, relative to the substrate, on the adhesion energy by translating the Cu layers in the $xy$ plane.

As shown in Fig 5, the adhesion energy turns out rather insensitive to the initial position of the Cu layers so long as the termination type remains unchanged. This result suggests that the adhesive properties realized in these $\alpha$-cristobalite substrates may well be carried over, to some extent, to those of glass substrates. The insensitivity of adhesion energy to the position of Cu layers does *not* imply that the detailed structure at the interface is less important for adhesion. In fact, as shown in Fig. 6 for the OO-terminated case, atoms at the interfaces *do* move significantly relative to the unshifted case. Since the surface atoms have a greater freedom to choose their position than those in bulk, the adhesion energy

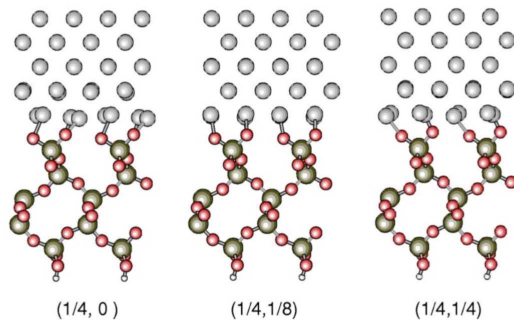


FIG. 6. (Color online) Structures at the OO-terminated interfaces obtained as a function of initial positions of Cu layers with respect to the substrate. The figures within brackets denote the shift of the position of Cu layers within the *xy* plane (see the caption of Fig. 5) in unit of 5 Å (the in-plane supercell lattice parameter).

remains rather constant for various initial positions of Cu layers.

### 2. Local oxygen surface coverage

Thus far we have investigated the Si, O, and OO terminations independently. Depending on the oxygen partial pressure, however, these terminations are generally expected to coexist on the substrate surface, independent of whether the substrate is crystalline or amorphous. To examine the effects of oxygen surface densities *intermediate* between those of the Si-, O-, and OO-terminated cases, we enlarge the supercell by a factor of two along the *y* axis (along the horizontal direction of Figs. 1, 2, and 6). For the $1\times2$ supercells, three new surfaces, in addition to those already considered above, are now possible. These are a (Si,O)-terminated surface which consists of neighboring Si- and O-terminated surfaces, a (Si,OO)-terminated surface which consists of neighboring Si- and OO-terminated surfaces, and a (O,OO)-terminated surface which consists of neighboring O- and OO-terminated surfaces. [Note that the (Si,OO)-terminated case possesses the same oxygen density as the O-terminated case.] We find that the (Si,OO)-terminated substrate has energy which is higher than that of the O-terminated surface by ~1.4 eV per Si atom at the surface (per 25 Å$^2$). Therefore, we restrict our focus to investigation of the (Si,O)- and (O,OO)-terminated cases, calculating their relaxed structures and adhesion energies.

Figure 7 depicts the adhesion energy as a function of the oxygen density at the interface. Remarkably, the adhesion energy is *not* a monotonically increasing function of oxygen density; at low oxygen density, increasing the number of O atoms a small amount does not necessarily lead to stronger adhesion. However, beyond the oxygen density of 4 nm$^{-2}$ where the OO termination will begin to appear appreciably, the adhesion energy increases, and does so almost linearly. This linear dependence implies that each OO surface unit contributes to the adhesion fairly independently, and thus the locally OO-terminated regions may not necessarily have to form large domains in order to work as an effective "glue," although it is clear that a critical density of such locally OO-terminated regions is required for strong adhesion.

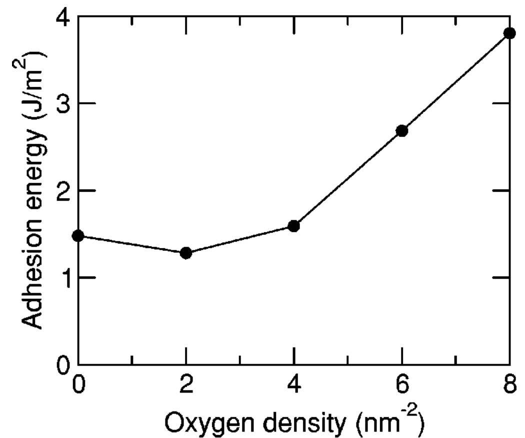


FIG. 7. Adhesion energy as a function of oxygen density at the substrate surface (Ref. 47). The densities 0, 2, 4, 6, and 8 nm$^{-2}$ correspond to the Si-, (Si,O)-, O-, (O,OO)-, OO-terminated cases, respectively.

### 3. Hydroxylated surfaces

We now address a frequently cited reason for the weak adhesion at Cu/$a$-$SiO_2$ interfaces, namely, the existence of hydroxyl groups on the $SiO_2$ surface.[7] It is well known that hydroxyls are likely to form on the $SiO_2$ surface under "wet" deposition conditions; to examine the impact of hydroxyls on adhesion from first principles, we add two hydrogens to the $1\times1$ OO-terminated surface, and relax all of the atoms. The result is that the cohesive energy of OHOH-terminated substrate, in which a Si atom is terminated by two hydroxyls, is lower than that of OO-terminated substrate by ~11.2 eV per surface Si atom. This energy difference is much larger than the dissociation energy of $H_2$ molecule (~4.5 eV per molecule), suggesting the high stability of the OHOH-terminated substrate. If we now place the Cu layers on top of the hydroxylated surface and relax the interface (Fig. 8), we find that the deposition of Cu layers does not significantly affect the structure at the OHOH-terminated surface, implying little interaction; the hydrogen present at the surface leaves the surface neutral and inert. This ten-

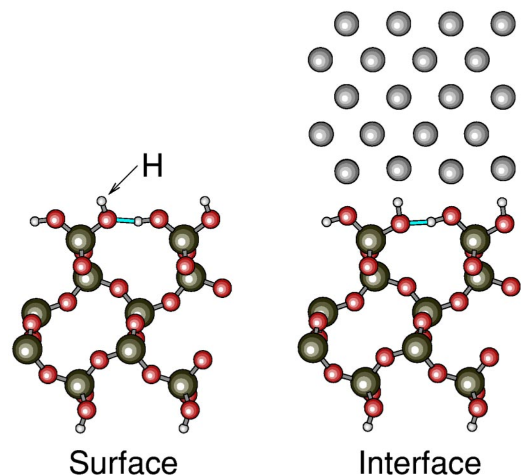


FIG. 8. (Color online) Relaxed structures of the OHOH-terminated surface and interface.

dency is clearly reflected in the calculated adhesion energy, and according to our calculations it is just 0.331 $J/m^2$, less than one tenth of the adhesion energy observed in the OO-terminated case.

However, as shown in Table II, the adhesion energies for all other cases studied here (i.e., the OO-, O-, and Si-terminated cases) seem to be of a magnitude which should produce adhesion, especially the oxygen-rich OO-terminated case. It is also noteworthy that the OO-terminated substrate, which has the largest adhesion energy among the three, looks actually the most stable substrate. These facts imply that should dehydroxylation of the substrate surfaces be successfully achieved (e.g., by annealing or particle bombardment of a growing film surface), robust adhesion is entirely possible, at least from the point of view of chemical bonding.

## V. CONCLUSIONS

We have performed a first-principles study of the adhesive properties of atomically sharp Cu/$SiO_2$ interfaces. As a model $a$-$SiO_2$ substrate, we used a crystalline polymorph of $SiO_2$, $\alpha$-cristobalite, and investigated its Si-, O-, and OO-terminated (001) surfaces in detail. For interfaces between Cu- and OO-terminated surfaces, a substantial rearrangement of oxygen positions relative to the free surface is observed, suggesting the formation of strong Cu-O bonds. Analysis of the local density of states at the interface showed that Cu-O interfacial bonds are composed of Cu-$d$ and O-$p$ states. The computed adhesion energy also exhibited a tendency toward much stronger adhesion in the OO-terminated interface than in the O- and Si-terminated interfaces: Substrate surfaces with high oxygen content were found suitable for adhesion. A future study obtaining adhesion energies within GGA would also be of significant interest, although we expect that our conclusions about the sensitivity of adhesion to the O density, and thus *relative* adhesion energies, will be largely unchanged by gradient corrections.

The adhesion energy is found to be very insensitive to the position of the Cu layers if the termination type is unchanged, and this observation suggests that $\alpha$-cristobalite may serve as a good starting model of $a$-$SiO_2$ substrates. The detailed dependence of the adhesion energy on oxygen density at the substrate surface has been investigated, and it shows that the surfaces where the O and OO terminations coexist can also lead to relatively strong adhesion.

The possible existence of hydroxyl groups at the substrate surface is thought to be the main cause for the weak adhesion observed in experiment. However, if these hydroxyls are removed beforehand and the oxygen density at the surface is increased (for example, by upping the oxygen partial pressure), Cu layers are predicted to adhere reasonably well to $SiO_2$. In addition to the possibility of direct comparison to future measurements on crystalline Cu/$\alpha$-cristobalite (001) interfaces, these results should serve as a starting point from which to study more complicated interfacial geometries, benchmarks for future investigations, and a baseline for experiments attempting to elucidate complicated phenomena affecting adhesion at Cu/glass interfaces.

## ACKNOWLEDGMENTS

We thank S. Baker and M. Backhaus for helpful discussions. This work was supported by the National Science Foundation (Grant No. DMR-9988576), and made use of the Cornell Center for Materials Research Shared Experimental Facilities, supported through the National Science Foundation Materials Research Science and Engineering Centers program (Grant No. DMR-9632275).

*Present address: Research Institute of Electrical Communication, Tohoku University, 2-1-1 Katahira, Aoba-ku, Sendai 980-8577, Japan.

[1] S.P. Murarka, Mater. Sci. Eng., R. **19**, 87 (1997).
[2] P. Benjamin and C. Weaver, Proc. R. Soc. London, Ser. A **261**, 516 (1961).
[3] D.M. Mattox, Thin Solid Films **18**, 173 (1973).
[4] A.J. Kellock and J.E.E. Baglin, in *Interfaces Between Polymers, Metals, and Ceramics*, edited by B.M. De Koven, R. Rosenberg, and A.J. Gellman, Mater. Res. Soc. Symp. Proc. No. 153 (Materials Research Society, Pittsburgh, 1989), p. 391.
[5] W.R. LaFontaine and C-Y. Li, in *Electronic Packaging Materials Science V*, edited by E.D. Lillie *et al.*, Mater. Res. Soc. Symp. Proc. No. 203 (Materials Research Society, Pittsburgh, 1991), p. 169.
[6] M.D. Kriese, N.R. Moody, and W.W. Gerberich, Acta Mater. **46**, 6623 (1998).
[7] T. Ohmi, T. Saito, M. Otsuki, T. Shibata, and T. Nitta, J. Electrochem. Soc. **138**, 1089 (1991).
[8] S.P. Murarka, R.J. Gutmann, A.E. Kaloyeros, and W.A. Lanford, Thin Solid Films **236**, 257 (1993).
[9] P.J. Ding, W.A. Lanford, S. Hymes, and S.P. Murarka, J. Appl. Phys. **75**, 3627 (1994).
[10] P.J. Ding, W.A. Lanford, S. Hymes, and S.P. Murarka, Appl. Phys. Lett. **65**, 1778 (1994).
[11] K. Shepard, C. Niu, D. Martini, and J.A. Kelber, Appl. Surf. Sci. **158**, 1 (2000).
[12] P-I. Wang, S.P. Murarka, G.-R. Yang, and T.-M. Lu, J. Electrochem. Soc. **148**, G78 (2001).
[13] P.F. Ma, T.W. Schroeder, and J.R. Engstrom, Appl. Phys. Lett. **80**, 2604 (2002).
[14] C.J. Liu, J.S. Jeng, J.S. Chen, and Y.K. Lin, J. Vac. Sci. Technol. B **20**, 2361 (2002).
[15] M. Hu, S. Noda, Y. Tsuji, T. Okubo, Y. Yamaguchi, and H. Komiyama, J. Vac. Sci. Technol. A **20**, 589 (2002).
[16] B.E. Warren, J. Appl. Phys. **8**, 645 (1937).
[17] P. Vashishta, R.K. Kalia, J.P. Rino, and I. Ebbsjö, Phys. Rev. B **41**, 12 197 (1990).
[18] S.H. Garofalini, J. Chem. Phys. **78**, 2069 (1983).
[19] B.P. Feuston and S.H. Garofalini, J. Chem. Phys. **89**, 5818 (1988).
[20] B.P. Feuston and S.H. Garofalini, J. Chem. Phys. **91**, 564 (1989).
[21] S.H. Garofalini, J. Non-Cryst. Solids **120**, 1 (1990).
[22] G.-M. Rignanese, A. De Vita, J.-C. Charlier, X. Gonze, and R. Car, Phys. Rev. B **61**, 13 250 (2000).
[23] S.V. Dudiy and B.I. Lundqvist, Phys. Rev. B **64**, 045403 (2001).

[24] I.G. Batyrev, A. Alavi, and M.W. Finnis, Phys. Rev. B **62**, 4698 (2000).
[25] J. Hoekstra and M. Kohyama, Phys. Rev. B **57**, 2334 (1998).
[26] D.J. Siegel, L.G. Hector, Jr., and J.B. Adams, Phys. Rev. B **65**, 085415 (2002).
[27] R.T. Downs and D.C. Palmer, Am. Mineral. **79**, 9 (1994).
[28] P. Hohenberg and W. Kohn, Phys. Rev. **136**, 864B (1964); W. Kohn and L.J. Sham, Phys. Rev. **140**, 1133A (1965).
[29] D.M. Ceperley and B.J. Alder, Phys. Rev. Lett. **45**, 566 (1980); J.P. Perdew and A. Zunger, Phys. Rev. B **23**, 5048 (1981).
[30] G. Kresse and J. Hafner, Phys. Rev. B **47**, R558 (1993); **49**, 14 251 (1994).
[31] G. Kresse and J. Furthmüller, Comput. Mater. Sci. **6**, 15 (1996).
[32] G. Kresse and J. Furthmüller, Phys. Rev. B **54**, 11 169 (1996).
[33] D. Vanderbilt, Phys. Rev. B **41**, 7892 (1990).
[34] G. Kresse and J. Hafner, J. Phys.: Condens. Matter **6**, 8245 (1994).
[35] P.E. Blöchl, Phys. Rev. B **50**, 17 953 (1994).
[36] G. Kresse and D. Joubert, Phys. Rev. B **59**, 1758 (1999).
[37] A.M. Rappe, K.M. Rabe, E. Kaxiras, and J.D. Joannopoulos, Phys. Rev. B **41**, 1227 (1990).
[38] R.W.G. Wyckoff, *Crystal Structures*, 2nd ed. (Interscience Publishers, New York, 1965) Vol. 1.
[39] For these calculations, the cutoff energy is increased up to ~38 Ry, and the $\boldsymbol{k}$-point number is set to $n_k = 10\times10\times10$ for fcc Cu and $n_k = 4\times4\times4$ for $\alpha$-cristobalite.
[40] R.T. Downs and D.C. Palmer, Am. Mineral. **79**, 9 (1994).
[41] A. Khein, D.J. Singh, and C.J. Umrigar, Phys. Rev. B **51**, 4105 (1995).
[42] D.M. Teter, G.V. Gibbs, M.B. Boisen, Jr., D.C. Allen, and M.P. Teter, Phys. Rev. B **52**, 8064 (1995).
[43] T. Demuth, Y. Jeanvoine, J. Hafner, and J.G. Angyan, J. Phys.: Condens. Matter **11**, 3833 (1999).
[44] J.P. Perdew, J.A. Chevary, S.H. Vosko, K.A. Jackson, M.R. Pederson, D.J. Singh, and C. Fiolhais, Phys. Rev. B **46**, 6671 (1992).
[45] J.B. Neaton, D.A. Muller, and N.W. Ashcroft, Phys. Rev. Lett. **85**, 1298 (2000).
[46] F. S. Galasso, *Perovskites and High $T_c$ Superconductors* (Gordon and Breach, New York, 1990), pp. 247ff.
[47] For these calculations, the $\boldsymbol{k}$-point number is set to $n_k = 4\times2\times1$ for the 5 Å×10 Å×30 Å supercell.